

**LNF-95/023**

## **First Operation and Perspectives of the Superconducting Linac LISA**

M. Castellano, M. Ferrario, M. Minestrini, P. Patteri, F. Tazzioli,  
F. Cevenini, L. Catani

*Nucl. Instr. & Meth. In Phys. Res. A 358, 331-333, (1995)*



ELSEVIER

# First operation and perspectives of the superconducting linac LISA

M. Castellano <sup>a,\*</sup>, M. Ferrario <sup>a</sup>, M. Minestrini <sup>a</sup>, P. Patteri <sup>a</sup>, F. Tazzioli <sup>a</sup>, F. Cevenini <sup>b</sup>,  
L. Catani <sup>c</sup>

<sup>a</sup> INFN-Laboratori Nazionali di Frascati, C.P. 13, 00044 Frascati, Italy

<sup>b</sup> INFN-Sezione di Napoli and Dip. di Fisica, Università di Napoli, Pad 20 Mostra d'Oltremare, 80125 Napoli, Italy

<sup>c</sup> INFN-Sezione di Roma II, Via E. Carnevale, Roma, Italy

## 1. Introduction

The first operation of the whole superconducting (SC) linac LISA has been carried out in March 1994. The beam has been accelerated by the four SC cavities to 18 MeV. The macropulse was 1 ms long with a current of 0.5 mA. The FEL activity is now in stand-by, although both the undulator and the optical cavity are installed or ready for installation at LNF, due to the involvement of the group in the TESLA Test Facility program. In this framework LISA will be mainly used as a test machine for SC accelerator studies and for the development of sophisticated diagnostic tools, exploiting the long macropulse and high average current not far from the TTF design parameters.

In this paper we review the achievements of LISA which could be of interest to the FEL community since a number of choices in the machine design, namely in the injector, were dictated by the FEL requirements.

## 2. Machine performances

### 2.1. The injector

The injector of LISA is composed of a 100 kV DC thermionic gun [1], a double transverse chopper at 50 + 500 MHz, a 500 MHz prebuncher and a 1 MeV capture section. The choice of this rather standard configuration instead of an RF gun was taken to concentrate efforts on the SC linac avoiding further task in developing a new injector. Nevertheless, the design specification, dimensioned for a future CW operation of the machine, implied the construction of a powerful low emittance long macropulse 1 MeV injector.

The injector operation now fulfills average current specifications, providing a 2 ms long macropulse at 2 mA of average current. The beam emittance has been measured both on axis after the 1 MeV capture section and after the U-turn bringing the beam on the axis of the SC linac. The measured emittance in both planes was  $\epsilon < 6 \times 10^{-7}$ , corresponding to normalized emittance  $\epsilon_n < 2 \times 10^{-6}$  at a current of 2 mA. The beam current and emittance measured along the injector are shown in Fig. 1.

The 1 MeV current at the exit of the capture section is measured before any bending magnet, so it was not surprising that a fraction of out-of-phase accelerated electrons with energy different from the main beam, contributing to current at CM3, was lost in the U-turn and was therefore missing in CM4. However, attempts to improve the transport obtained 100% efficiency in some part of the macropulse and much lower in the remaining part, causing a triangular shape of the macropulse. This meant that a variation of parameters along the macropulse affected the capture efficiency and acceleration in the 1 MeV preaccelerator. The position of the transport efficiency peak was found depending on the phase of the prebuncher and on the gun HV. This indicated that voltage drop due to beam loading in the gun power supply allowed for an optimal matching of bunching parameters only for a few hundreds of microseconds; upgrading of the gun HV supply improved the transport efficiency to  $> 80\%$  and provided a nearly rectangular pulse shape. The last step was the proper setting of the feedback to keep a stable phasing between input power to the capture section and beam; the feedback input is taken from the input power since a pick up sensing the field inside the cavity is not available, however this proved to work effectively raising the transport efficiency up to 100%; a typical shape of the correction signal applied to the phase shifter is shown in Fig. 2; the phase correction applied between the center and the end of the pulse is  $\sim 15^\circ$ .

When routine operation of the machine achieved these performances we were able to use the optical transition

\* Corresponding author. +39 69 40 32 10, fax +39 69 40 35 65.

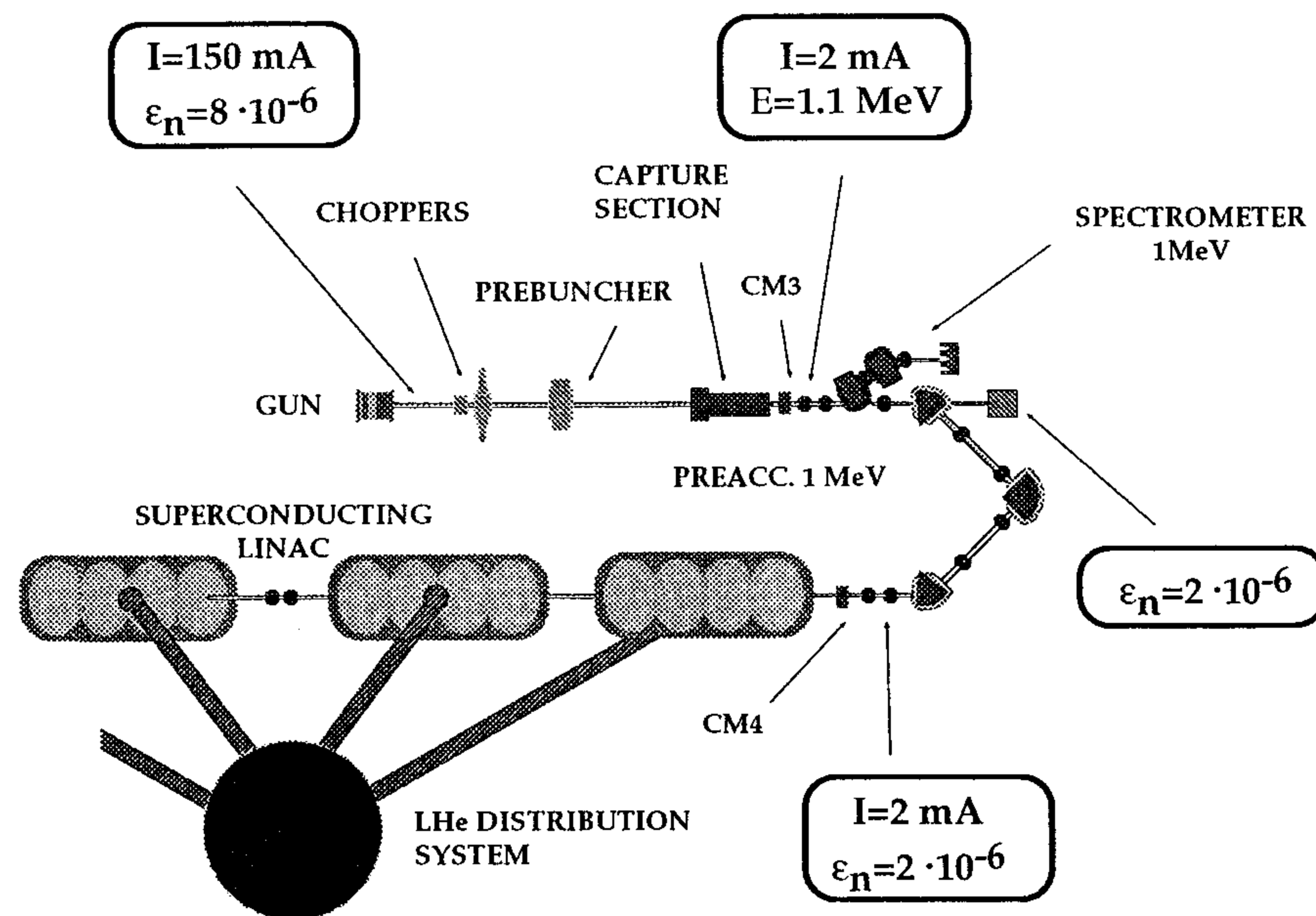


Fig. 1. Schematic layout of LISA.

radiation at 1 MeV to carry out systematic measurement of the beam size [2,3].

## 2.2. The superconducting linac

The operation of the superconducting cavities was obtained for the first time in November 1992. The LISA cavities are strongly coupled to the RF generator to accelerate a high average current in a long macropulse; tuning and locking the cavities within the narrow bandwidth  $\sim 200$  Hz is obtained with a fast electronic phase feedback and a slow mechanical tuning.

In order to reduce the thermal load to the refrigerator the rf power is pulsed. The repetition rate is usually 1 Hz, at a duty cycle  $\sim 2\%$  in beam operation mode, and 25% for conditioning. The pulses are added over a continuous low level drive signal, which helps keeping the tuning locked. A very slow frequency drift (about a few Hz/s) is observed if this feedback is turned off, allowing measurements of beam induced effects on a tuned but unpowered cavity.

The SC cavities were put in operation after a two years long inactivity and without a power conditioning at the construction site. The accelerating field was initially limited to  $< 3$  MeV/m by strong electron emission, evidenced by the intensity of X-rays outside the cavities, but after a few hours of RF conditioning the emission decreased and the cavities safely sustained fields of 4–4.5 MeV/m.

Although the large coupling factor to the generator makes the measurement of the quality factor  $Q_0$  rather cumbersome [4], systematic measurements showed that  $Q_0$  increased during the RF conditioning. Further improvement with respect to the first cooldown have been measured after the last two shifts of operation. This indicates that the best cleaning of the inner surface is not yet achieved; however the average accelerating field now exceeds the design value of 5 MeV/m and the  $Q_0$  vs  $E_{acc}$  behavior is better than those measured soon after the construction.

The beam transport and acceleration through the superconducting linac was readily obtained in November 1993 with only the first accelerating module powered. In two further shifts in March and May 1994 all the accelerating modules were put in operation simultaneously and phased

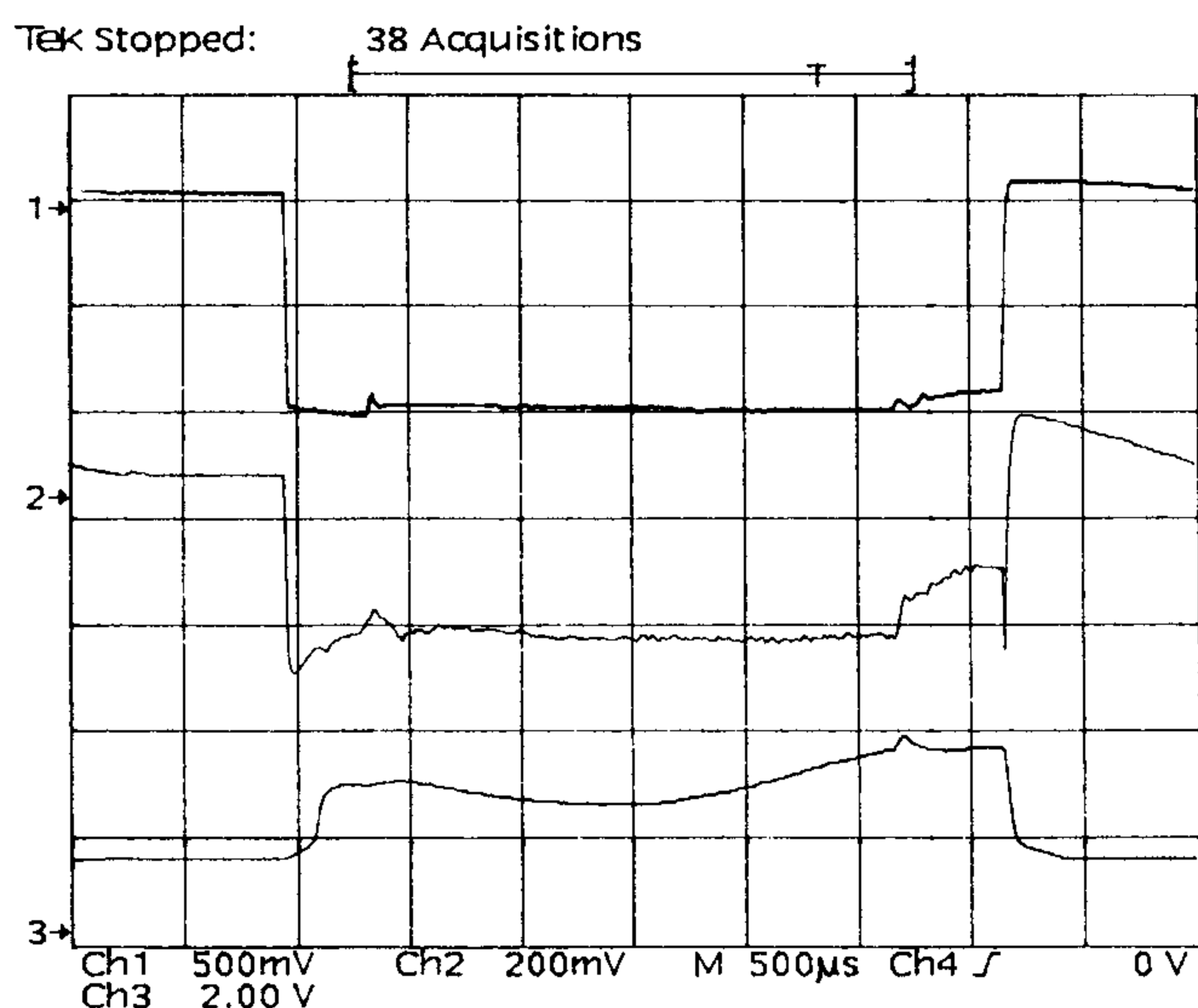


Fig. 2. Plots of the forward power (curve 1), reflected power (curve 2) and phase correction signal at  $15^\circ/\text{V}$  (curve 3) during the capture section rf pulse.

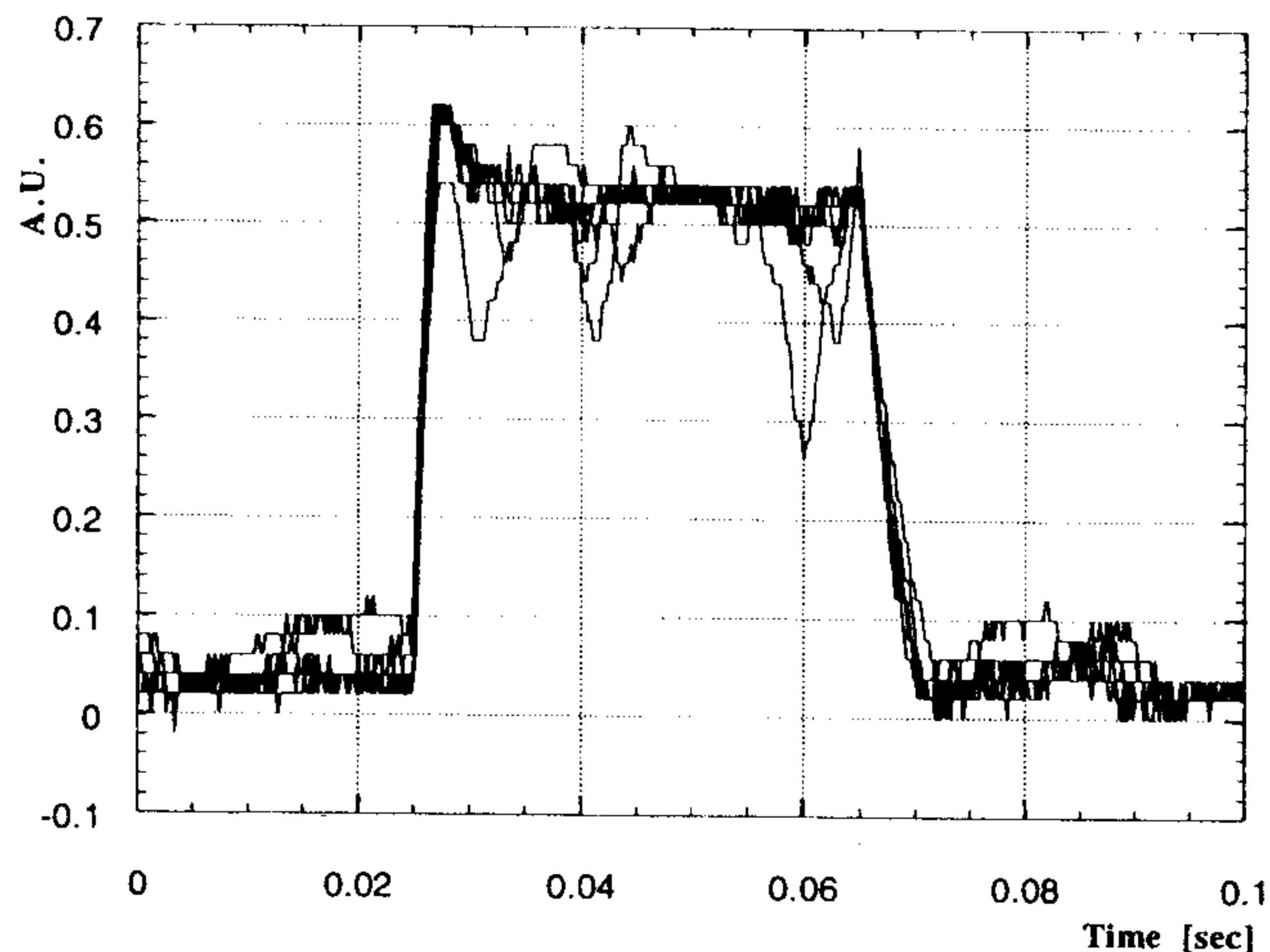


Fig. 3. RF level oscillation in a perturbed SC cavity.

for acceleration up to a final energy of 18 MeV. The beam transport efficiency from one module to the next was improved by maximizing the beam induced signal in the following unpowered module. An accelerated current of  $\sim 0.5$  mA was measured both by the resistive wall current monitor at the linac exit and by the field induced in the last cavity with no RF power input.

Optical and electrical measurement at the linac exit are now disturbed by a strong dark current coming from the last two cavities, which had a shorter conditioning time. This current has of course a much lower energy and a wider direction distribution with respect to the accelerated beam so that it is strongly affected by the focusing and steering elements at the SC linac exit. Measurements are made difficult both by the fluorescence light and the X-ray emission caused by the electrons impinging on the inner vacuum pipe; although a decrease of dark current emission has been already observed, more shieldings are planned to counteract this background.

The main limit to regular operation is the random onset of RF level oscillation, as shown in Fig. 3, apparently related to the average level of He pressure on the LHe bath. A measurement of the vibration spectra rejected the hypothesis of perturbations due to a thermoacoustic oscillation because no well defined line was found; moreover, no significant change of the spectrum was observed changing the length of some potentially resonating structures.

We suspect now that this effect is due to an unstable equilibrium of the cryogenic system as a whole, since this phenomenon, at the beginning apparently more frequent for the cavities 1 and 4, which are farthest from the LHe distribution valve box, showed in the following a tendency to flip randomly from outer to inner cavities. Further work is planned to study this effect more deeply.

### 3. Diagnostics upgrading

OTR based diagnostics will be extensively used at TTF both for high resolution beam profile and for time resolved measurements. The equipment to be used in the 500 MeV line of the TTF will be developed at LNF and previously tested both with LISA and with the 500 MeV injector for the storage ring Dafne. Two systems with design performances defined by different trade-offs between time and spatial resolution are under construction. The fastest diagnostic system is based on a  $16 \times 16$  multianode PMT, followed by a LeCroy FERA charge sensitive ADC system capable of observing the beam evolution during the macropulse at a sampling rate of 40 frame/ms. The slower will be based on a CCD linear array of  $\sim 1000$  pixels; it will provide a detailed section of the OTR emission integrated over a minimum time of  $\sim 50$   $\mu$ s; this performance will make the device useful for time resolved energy measurements at the spectrometer.

The PMT has been intended for high gain, low rate counting per pixel and its biasing is not suited to operation at high repetition rate for rather long time,  $\sim 1$  ms; this asks for a careful optimization of the illumination and gain to avoid exceeding the overall average current limit of 100  $\mu$ A. At such a low current in the maximum gate opening of 1  $\mu$ s the integrated charge per pixel, with a uniformly illuminated cathode, is  $\sim 1$  pC, corresponding to only 4 counts of the ADC. Since digitizing and readout last  $\sim 25$   $\mu$ s, the current at each anode is integrated on a capacitor during this period and the accumulated charge is then reversed, closing an analog switch, in the ADC input during the 1  $\mu$ s gate opening, exploiting at the best the whole dynamical range of the ADC.

Simple Monte Carlo simulations, taking into account any known noise source, have been carried out looking for the best trade-off between the wider field of view and beam position resolution. Assuming that the spot imaging on the PMT photocathode is done so that its  $\sigma$  corresponds to 2 pixels of the cathode grid, a resolution of  $0.01\sigma$  can be obtained for its center position.

### References

- [1] M. Castellano et al., Nucl. Instr. and Meth. A 332 (1993) 354.
- [2] M. Castellano et al., Beam diagnostics with OTR at the SC Linac LISA, presented at the 4th Europ. Particle Accelerator Conf., London, 27/6–1/7 1994.
- [3] M. Castellano et al., Analysis of optical transition radiation emitted by a 1 MeV beam and its possible use as diagnostic tool, to be published in Nucl. Instr. and Meth.
- [4] M. Castellano et al., Nucl. Instr. and Meth. A 332 (1993) 347.